Accepted Manuscript

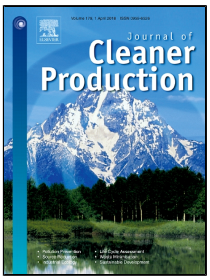

The deterioration and environmental impact of binary cements containing thermally activated coal mining waste due to calcium leaching

I. Arribas, I. Vegas, V. García, R. Vigil de la Villa, S. Martínez-Ramírez, M. Frías

PII:	S0959-6526(18)30439-6
DOI:	10.1016/j.jclepro.2018.02.127
Reference:	JCLP 12074
To appear in:	*Journal of Cleaner Production*
Received Date:	24 October 2016
Revised Date:	11 February 2018
Accepted Date:	13 February 2018

Please cite this article as: I. Arribas, I. Vegas, V. García, R. Vigil de la Villa, S. Martínez-Ramírez, M. Frías, The deterioration and environmental impact of binary cements containing thermally activated coal mining waste due to calcium leaching, *Journal of Cleaner Production* (2018), doi: 10.1016/j.jclepro.2018.02.127

The deterioration and environmental impact of binary cements containing thermally activated coal mining waste due to calcium leaching

I. Arribas[a], I. Vegas[a], V. García[a], R. Vigil de la Villa[b], S. Martínez-Ramírez[c], M. Frías[d],

[a] Tecnalia, Parque Tecnológico de Bizkaia, 28160 Derio, Spain

tel.: 902 760 000, fax: 944 041 445

email: idoia.arribas@tecnalia.com

[b]Dpto de Geología y Geoquímica, Unidad Asociada CSIC-UAM, Universidad Autónoma de Madrid, 28049 Madrid, Spain

[c]Institute for the Structure of Matter (IEM-CSIC), 28006 Madrid, Spain

[d]Eduardo Torroja Institute for Construction Science (CSIC) 28033 Madrid, Spain

Abstract

Calcium-leaching processes can potentially degrade the structure of a concrete matrix. This problem is studied here through the progressive dissolution of Ca^{2+} in both ordinary Portland cement pastes (C-0) and binary cement blends (C-20) containing 20% thermally Activated Coal Mining Waste (ACMW)[1]. A series of accelerated tests are conducted that involve the immersion of these cement pastes in a 6 M ammonium nitrate solution at a temperature of 20ºC for 7 and for 21 days. A rise in paste porosity was observed, due to increased capillary pore sizes of between 5 and 0.1 microns. In the case of the 20% ACMW pastes (C-20), calcium leaching decreased, probably as a consequence of the pozzolanic effect of the ACMW, while potassium and magnesium leaching increased, due to the presence of the phyllosilicates in the ACMW. The paste compounds most

[1] ACMW, activated coal-mining waste

affected by leaching were $Ca(OH)_2$, $C_6AS_3H_{32}$, and $C_4A\overline{C}H_{12}$. In general terms, it can be concluded that the incorporation of ACMW into binary cements slightly reduces the calcium leaching phenomena. Concerning the environmental impact assessment, the substitution of 20% OPC by ACMW reduced CO_2 emissions by as much as 12% and improved energy efficiency by using approximately 19% fewer fossil resources.

Keywords

Calcium leaching, thermally activated coal mining waste, binary cements, degradation.

1. Introduction

One of the problems of Portland cement concrete is its poor durability in the presence of certain aggressive agents, among which those with a high calcium oxide content. The cement matrix will deteriorate in the presence of pure water and in any other environment that produces calcium lixiviation. This phenomenon is attributed to the dissolution of calcium ions (principally from calcium hydroxides and ions from CSH gels). The decalcification of concrete elements and structures that remain in contact with pure or acidic waters over long periods of time can be affected, as in the case of water pipes and cisterns, dams, and even nuclear waste storage facilities. As the lixiviation of calcium oxide progresses, the cement matrix shows increasing porosity that leads to a loss of its mechanical strength and functionality.

The hardened cement paste consists of Portlandite, calcium aluminate hydrates and unhydrated clinker embedded in calcium silicate hydrate gel (C–S–H) (Taylor, 1997). This heterogeneous structure induces porosity within the cement paste where dissolved calcium minerals are deposited. Consequently, the exposure of the cement matrix to any aggressive environment with a pH lower than 12.5, such as 6M ammonium solution, leads

to its progressive dissolution, due to the migration of the calcium ions from the matrix to the solution (Gaitero et al 2008). This degradation mechanism of the cement matrix is known as calcium leaching.

According to Goñi et al (2013), the calcium leaching of cement pastes depends on different factors: the solubility of the hydrated compounds, the type of cement, the Ca/Si ratio, the nature of the pozzolan, and, finally, the pozzolanic rate. According to other researchers, it is also related to the presence of dissolved organic matter, pH, and redox reactivity (Medina et al., 2014; Mulugeta et al., 2011). The degradation of the hydrated compounds of the cement matrix is related to the Ca/Si ratio in the pore solution. Portlandite degradation starts when the calcium concentration in the pore solution is lower than 20 mol/m^3, with equilibrium values for the C–S–H gel ranging between 2 and 20 mol/m^3 (Berner, 1988). The C-S-H gels dissolve to yield a progressive homogenization of the paste with a lower Ca/Si ratio, while the Portlandite is completely broken down to Ca^{2+} and OH^-, leaving a network of pores in its place. Porosity and permeability increase, lowering the mechanical strength of the cement matrix (Gaitero et al., 2008). The positive advantages of incorporating pozzolanic material in Portland cement that can resolve and reduce the aforementioned effects are well known (Taylor, 1997; Juenger and Siddique, 2015; Nakanishi et al., 2016). The composition and Ca/Si ratio of the C-S-H gels that form in those blended cements differ from those found in plain OPC (Sáez et al., 2014).

Among other materials such as slag [Santamaría et al, 2016] and GGBS, metakaolin, is well known as a supplementary cementitious material that reduces the environmental impact of the Portland clinker manufacturing process and increases the mechanical performance of cement materials and their durability. Over the past few years, industry has been demanding alternative sources for MK, given the ever-greater constraints on the exploitation of natural kaolinite quarries. A cleaner technology for the production of MK

involves with the controlled thermal activation of deinking paper sludge and carbon mining waste. An abundance of research and investigation has already demonstrated that the controlled calcination of those waste streams can manufacture a highly reactive MK-containing pozzolanic material, within a temperature range of between 600 and 750ºC. Recent research works have mainly focused on Activated Carbon Mining Waste (ACMW) in substitution of OPC (Frías et al., 2016; Rashad, 2013). Despite scientific progress, there is still an important gap with regard to the behavior of these new matrices in relation to lixiviation processes.

Hence, the main purpose of this paper is to study the influence of this pozzolanic addition on the decalcification process of both a binary cement paste (C-20) and a plain OPC paste (C-0), by examining the leaching behavior of the calcium ions. Excessively lengthy time periods are needed to obtain uniformly leached specimens when studying the impact of calcium leaching on cementitious materials. Calcium leaching in deionized water, the most common aggressive solution in industrial applications, is dependent on diffusion. The leaching rate is therefore extremely slow, at roughly 30 μm/year. Some accelerated method is therefore needed to reach a certain stage of degradation that is comparable to the long-term damage of natural leaching. Unlike other aggressive environments (freeze/thaw, sulfate attack, and chloride penetration) for concrete, calcium leaching is not standardized and its study is based on previous research works. Two different accelerated methods were found in the literature. The first one consists of applying a strong electrical field to the sample (Saito, 1992 and Gerard, 1997). As a consequence, a migration of Ca ions of the pore solution towards the cathode occurs, which induces a calcium deficit in the solution and the dissolution of cement hydrates. This method is not driven by diffusion, so the nature of accelerated leaching differs from real conditions. In addition, this method leads to an inhomogeneous decalcification of the cementitious

paste, as a function of the distance between the anode and cathode, as well as the strength of the electrical field. The second and the most popular accelerated method, recently (2014-2017) published in previous studies (Gaitero et al., 2008 and Phung, 2015), consists of replacing the deionized water with an ammonium nitrate solution. The higher solubility of calcium in this solution leads to faster degradation, when compared with other methods under diffusive-transport conditions, with the same end-products. Although contact between concrete structures and ammonium nitrate does not represent real operative conditions, a 6M ammonium nitrate solution was used in the present work that accelerates the Ca-leaching degradation kinetics, as explained earlier.

2. Materials and methods

2.1. Materials

The Coal Mining Waste (CMW) was supplied by the Spanish Coal Group, Sociedad Anónima Hullera Vasco-Leonesa, located in the province of León. ACMW was produced in the laboratory by heating the CMW at 600ºC for 2h, as described in previous research works (Frías et al., 2011; Frías et al., 2012). The OPC (CEM I 52.5N) was provided by Financiera y Minera (Italcementi Group). The physical properties and chemical composition of both the CEM I and the ACMW are given in Table 1. The chemical composition was determined by X-ray fluorescence (XRF) using a Philips PW 1404 and an Sc-Mo X-ray tube, while both fineness and particle size distribution were determined by means of laser diffraction (LRD), using a Sympatec Helos 12 KA spectrometer and isopropyl alcohol as a non-reactive liquid (Frías et al., 1991)

The mineralogy of ACMW mainly consists of quartz, mica, hematite, and calcite, while the kaolinite is completely transformed into metakaolin. Further details on mineralogical changes were presented in a previous work (Frías et al., 2011). The cement has the

standard Bogue composition of type I Portland cement with 45wt% C_3S, 24wt% C_2S, 10wt% C_3A, and 10wt% C_4AF, in accordance with the Bogue equation to determine the chemical composition of cement.

Binary cement blends (C-20) were prepared by partially replacing OPC (CEM I 52.5N) with thermally activated CMW (at lab scale) at 600ºC for 2h (ACMW), according to previous works (Frías et al., 2011; Frías et al., 2012). Binary blends were prepared by replacing 20% of the OPC with ACMW at a water/binder ratio (w/b) of 0.5. An OPC mix, without ACMW, was also prepared for comparison (C-0).

2.2. Methods

2.2.1. Leaching test

In accordance with the experimental methodology reported in previous studies (Gaitero et al., 2008 and more recently, Phung, 2015), prismatic cement paste samples of 1×1×6 cm^3 were cast, according to the EN 196-1 standard (UNE EN 196-1). The samples were cured for 24h in a chamber at 20°C and 100% relative humidity. They were then demolded and submerged in a saturated lime solution, to avoid calcium loss over the remaining 27 days of curing. Subsequently, they were immersed in 6M ammonium nitrate solution (Saito et al., 1992) that increases the imbalance and consequently the dissolution rate. The slow kinetics of leaching with ionized water increased under the aggressive conditions associated with ammonium nitrate. The degradation process involves dissolution followed by a diffusion process and a strongly homogenized solution was necessary. The tests were performed at 7 and at 21 days after immersion in the aggressive solution, because the rapid dissolution of Portlandite and the slow decalcification of the C–S–H gel had to be studied at separate points of time (Gaitero et al., 2008). Several

different techniques were used, due to the complexity of the reactions under study, to characterize the cementitious materials:

2.2.2. Inductively coupled plasma mass spectrometry (ICP-MS).

The concentration of the aqueous species of interest (Na, K, Mg, Ca, Al and Si) were measured in an aqueous solution by ICP-MS with an Elan 6000 Perkin–Elmer Sciex analyzer.

2.2.3. X-ray fluorescence (XRF)

The chemical characterization of the oxides was performed by XRF, using a Philips PW 1404 and an Sc-Mo X-ray tube.

2.2.4. X-ray diffraction (XRD)

The mineralogical characterization of the bulk samples was determined by means of a random powder XRD on a Siemens D-500 (Munich, Germany) X-ray diffractometer fitted with a Cu anode. The operating conditions were as follows: 30 mA and 40 kV and 2 and 0.6 mm divergence and reception slits, respectively. The samples were scanned in (2θ) 0.041 steps with a 3s count time.

2.2.5. Scanning electron microscopy (SEM/EDX).

The morphological characterization was carried out by using a SEM/EDX, FEI microscope, model "Inspect" Quanta 200.

2.2.6. Fourier Transform Infrared Spectrometry (FTIR)

Specimens were prepared by mixing 1mg of sample in 300 mg of KBr. Spectral analysis was performed over a range of 4,000–400 cm^{-1} at a resolution of 4 cm^{-1} on an Ati Mattson FTIR-TM series spectrophotometer.

2.2.7. Flexural and compressive strength

The equipment used for this test was customized to meet the requirements of the samples in terms of dimensions and strength according to the standard procedure (UNE EN 196-1), but on a smaller scale.

2.2.8. Porosity and pore size distribution

Porosity and pore size distribution in C-20 were measured by using a Micromeritics Autopore IV 9500 mercury intrusion porosimeter (MIP) at a pressure of 227.5 MPa, sufficient to determine pore sizes of up to 0.0067μm. The mercury contact angle was 141.3ºC.

2.2.9. Environmental assessment

A comparative Life-Cycle Analysis (LCA) between a plain OPC paste and a binary cement paste with 20% of the OPC replaced by ACMW was performed, with a view to the assessment/quantification of the environmental impact. The LCA methodology used in this study is based on international standards ISO 14040, 14044 (ISO 14040 2006). The data for preparing the Life-Cycle Inventory (LCI) were taken from the European Life Cycle data base (ELCD 3.2 2015) and from different sources relating to coal mining waste.

2.2.9.1. *Goal and scope definition.* The goal of this LCA was to understand the environmental performance of a binary cement paste (C-20) versus a plain OPC paste (C-0). The study was focused on a cradle-to-gate assessment. It should be clarified that the use and the end-of-life phases were not included within the system boundaries. A flow chart of the binary cement production is shown in Figure 1, reporting the system boundaries and the manufacturing phases. 1 ton of the product was selected as the functional unit (F.U), for the comparison between C-20 and C-0,

2.2.9.2. *Life cycle inventory.* The data for OPC production were provided from the ELCD 3.2 (ELCD 3.2 2015). This process includes raw material extraction, raw material

preparation, and the clinker manufacturing process. Some assumptions were considered when assessing the production of 1 tone of ACMW, given that sufficient data could not be found within available databases, as this material cannot be found in databases. The thermal energy needed for the industrial calcination of the CMW was estimated, taking into account the average heat consumption for clinker manufacturing in the EU industry (3,74GJ/t clinker) (WBCSD/CSI, 2013) and the temperature difference to obtain both. However, the thermal energy was exceeded, due to the calorific power of the CMW (2000MJ/t of CMW) (Vadillo Fernández 1995), and the generation of energy could even be considered.

The CO_2 emissions emitted during the calcination process of the CMW were quantified, by taking into account that 8% of the CMW is combustible material (Vadillo Fernández 1995). The electrical energy required for grinding the calcined CMW was calculated in accordance with Bond's law, applying Bond's work index and assuming a reduction in grain size from 5mm to 15µm, which is the average particle size of conventional cements (Marchese García 2004).

2.2.9.3 Impact assessment. The results of the LCI are linked to specific environmental impact categories, in the Life Cycle Impact Assessment (LCIA), in order to predict potential environmental impacts related to the system under study. LCIA was conducted by using the midpoint assessment developed by Centre of Environmental Science (CML), Leiden University (Guinée et al. 2002). The impact categories under evaluation were resource depletion, due to the intensive use of raw materials and fossil fuels, acidification, eutrophication, global warming potential and photochemical oxidation, due to the atmospheric emissions from the cement kiln and other emissions associated with electricity generation, transport, and ozone depletion. The results obtained at the end of

the LCA analysis were intended to demonstrate improvements in environmental impact when using a binary cement containing 20% ACMW.

3. Results and discussion

3.1. Leaching Test

The results of the concentration measurements of several elements in the leachate between day 0 and day 21 are shown in Figure 2. The values for aluminum and silicon remained almost constant below the value of 2 mg/l. The decrease in Al and Si concentrations at 21 days was due to the incorporation of Al and Si in the C-S-H and the $C_3ASO_4Ca12H_2O$ phases that were formed. The presence of Al in the dissolution of the cement matrix decreased with increased exposure. This fact could be attributed to the incorporation of Al into the structure of the C-S-H gel and its modification. Sodium and magnesium showed variations in their concentrations within the range of 10 to 20 mg/l over the period from day 7 to day 21. However, potassium and calcium revealed more interesting variations. The concentrations of potassium in the leachate C-0 and C-20 hardly showed differences after 7 days exposure (70 mg/l in C-0 and 82 mg/l in C-20), while the potassium content clearly decreased (from 82 to 45 mg/l) after 21 days in C-20, remaining almost constant (75 mg/l) in C-0. The presence of ACMW, containing mainly metakaolin and other minerals, induced an initial increase in the potassium content (from day 0 to day 7) and then a final decrease. This evidence can be attributed to the dissolution of phyllosilicates, which are mineral phases containing Na and K (García et al., 2015). The calcium content in the leachate is strongly marked and relevant in both cases. For C-0, the calcium content increased to 7.3 g/l between day 0 and day 7, and then, from day 7 to 21 it also showed a considerable increase up until 9.8 g/l. The dissolution of calcium was quick over the first few days, slowing down over the two following weeks. The evolution in the leachate of C-0 was quite similar to that of C-20 paste from day 0 to day

7. However, in the case of C-20, from a content of 7 g/l on day 7 the concentration registered a decrease of 4.2 g/l after two weeks. Under real conditions of concrete exposed to low pH water, the water rarely remains stagnant and the real evolution might differ from the accelerated test. If the real phenomenon is similar to these tests, the apparent benefit of calcium decreasing after day 7 in paste C-20 would be rendered useless, due to the permanent renewal of water. The correlation between real and accelerated tests will require further research. The evolution of calcium concentrations from day 0 to day 7 was quite similar in both leachate pastes. Nevertheless, the concentration of calcium in C-20 decreased after two weeks compared with the concentration in C-0. The cumulative concentration of calcium ions in C-20 at 21 days should have been higher than that found at 7 days as a consequence of the degradative effects. This drop in the concentration values of calcium ions for C-20 could be attributed to the precipitation of calcium ions under acidic conditions. In any case, C-20 showed a lower degradation in calcium leaching when compared to C-0, given that C-20 showed more polymerized gels.

An element of the leachate in both C-0 and C-20 was observed in the FTIR spectrum, as discussed in section 3.2. The concentration of all elements in C-20, decreased with increased exposure to low pH water.

3.2. Solid Samples Test

3.2.1. XRF

With a view to the evaluation of the leaching effect on the chemical composition of both cements (C-0 and C-20), the major oxides were quantified by XRF for each time frame. Table 2 lists the contents of the major oxides at days 0, 7, and 21 of the accelerated leaching test. The results revealed a progressive decrease in the CaO content of both cements as the exposure time was increased. C-0 also evidenced a reduction in lime

content to around 44.5% at 21 days exposure, while in the case of C-20 it was around 54.5%. Potassium oxide content decreased in the C-0 mix, but not in the C-20 mix. However, C-20 showed a higher decrease in sodium oxide content as a consequence of the accelerated calcium leaching. As a result of this process, the CaO/SiO_2 ratio decreased over lengthier exposure times (Table 3); reductions of 69% and 71% were detected for C-0 and C-20, respectively.

The calcium leaching behavior when using an aggressive dissolution of ammonium nitrate was not in line with previous works by Goñi et al (2013) on leaching cement matrices containing 21% fly ash and activated paper sludge in pure water. Those authors reported a slower descaling process in blended cement paste than in the C-0 paste.

3.2.2. XRD

The XRD analysis for both C-0 and C-20 paste showed, in all cases, the following crystalline hydrated phases produced as a function of the replacement percentage (Figure 3): a) Portlandite with reflection peaks at [4.90Å (18.10 2θ), 3.11Å (28.17 2θ), 2.62Å (34.22 2θ), 1.92Å (47.34 2θ), 1.79Å (51.02 2θ) and 1.68Å (54.62 2θ)]; b) ettringite ($C_6AS_3H_{32}$) at [9.73Å (9.08 2θ), 5.61Å (15.78 2θ), 3.88Å (22.92 2θ), 2.56Å (35.04 2θ), and 2.20Å (41.02 2θ)]; c) (C_4AH_{13}) at [8.17Å (10.82 2θ), and 2.88Å (31.04 2θ)]; and, d) in the spaces between 7.60Å (11.64 2θ) /7.56Å (11.70 2θ) and 3.85Å (23.,10 2θ) /3.80Å (23.40 2θ), the diffraction peaks corresponded to the (0001) and (0002) layers for the $C_4A\overline{C}H_{12}$. Portlandite is the most common hydrated phase and ettringite is the second most abundant hydrated phase. However, the formation of $C_4A\overline{C}H_{12}$ and C_4AH_{13} differed: $C_4A\overline{C}H_{12}$ formation was favored in C-0, while C_4AH_{13} formation was favored in C-20 (Figure 3).

The leaching of ions (mainly calcium and hydroxide) from the pore solution to the external environment determines the dissolution of those hydrates. This phenomenon

typically affects structures which are in contact with the aggressive solution. It is well known that $Ca(OH)_2$, $C_4A\overline{C}H_{12}$, and C_4AH_{13} are the first hydrated phases to be dissolved, given that they are the most soluble of the hydrated compounds (Goñi et al., 2013).

A decrease in $Ca(OH)_2$ and $C_4A\overline{C}H_{12}$ and an increase in $CaCO_3$, $C_6S_3H_{32}$, and $C_3ASO_4Ca12H_2O$ was observed after 7 days exposure of the OPC sample. After 21 days, the gradual elimination of $Ca(OH)_2$ and $C_6S_3H_{32}$ and the increase of quartz and calcite continued. At that time, the reflections were undetected. The replacement of 20% of the OPC by ACMW promoted both the formation and the elimination of Portlandite that disappeared completely after 21 days (Fig 3).

3.2.3. SEM

An abundance of C-S-H gels, $Ca(OH)_2$ plates, and $C_6S_3H_{32}$ prisms was observed in the internal area of C-0, by means of SEM. The degradation of the material was more predominant in the external area of the C-0. The surfaces of the sheets became porous and the edges of the crystals were poorly defined, displaying the beginning of superficial degradation. The leached material from gels and Portlandite was deposited in the holes and pores of the previously formed degraded surfaces. Gypsum sheets were also observed (Figure 4), due to the dissolution of ettringite and the latter reaction between sulfate ions and calcium ions.

Both the C-0 and the C-20 samples underwent similar degradation following their immersion in the aggressive solution, although in the case of C-0 it was more pronounced. Amorphous forms from leached materials were deposited in the holes and pores formed on the degraded surfaces of the laminar structures (Figure 5a). Laminar $C_3ASO_4Ca12H_2O$ was also observed (Figure 5b). This fact might have caused the decrease in leaching related to C-20.

3.2.4. FTIR

Figure 6 shows the IR spectrums before and after the leaching process. The reference C-0 (black line) presented the strongest signal at 980 cm-1, which can be assigned to Si–O stretching vibrations of the Q2 tetrahedra in the C-S-H gel (Yu et al., 1999). After the leaching process of C-0 (21 days) a displacement of the band to higher frequencies, 994 cm^{-1}, was evidenced. According to Bjornstrom and Mollah et al (Bjornstom et al., 2004; Mollah et al., 2000), the shifting of the Si-O asymmetric stretching vibration (ν3 at 952 cm^{-1}) towards higher wave numbers in the cement hydration indicates polymerization of the silicate units.

In the case of C-20, the C-S-H gel presented the maximum vibrations, ν_3, at values higher than the initial C-S-H gel, with a small shift to higher frequencies after the leaching.

So, C-20 initially presented a more polymerized gel and it was less modified by the leaching process than C-0. Similar results were obtained by Gaitero et al (2008), who observed that the pozzolanic addition (nanosilica) caused a decrease in calcium leaching, induced by structural modifications of the C-S-H gel. Generally, as the polymerization of the C-S-H gel increased, there was a decrease in the Ca/Si ratio.

It is worth highlighting that the reference cement presented a broad band at 811 cm^{-1} that increased in intensity as the Ca/Si ratio increased, which can be assigned to Si–O stretching of Q1 tetrahedra. This finding also confirmed the polymerization of both the reference cement after lixiviation and the blended cement before and after lixiviation.

3.3. Mechanical strength

Figures 7 and 8 illustrate the evolution of flexural and compressive strength of C-20 and the reference C-0, respectively.

An increase of about 10% in flexural strength, induced by the pozzolanic effect of the ACMW, was appreciable after 28 days of curing. 7 days after the degradation started, C-0

had undergone greater degradation with a 76% reduction while C-20 presented reductions of about 72%. The difference between C-20 and C-0 was smaller as the degradation worsened, in such a way that after 21 days of exposure, C-0 revealed a reduction of about 84%, while C-20 presented reductions of about 82%, rising to similar values of flexural strength, in both cases at the end of the study.

A decrease of 28% in compressive strength was observed compared to C-0. This difference only became smaller after 7 days of degradation, because C-0 had undergone greater degradation with a 67% reduction in compressive strength, while C-20 presented reductions of about 54%. After 21 days of exposure, both cement matrices, C-0 and C-20, experienced a compressive strength reduction of approximately 85%.

3.4. Porosimetry

Total and partial porosities and pore size distribution were analyzed by mercury porosimetry, in order to determine the effect of the leaching process on the porous structure of both cement matrices (C-0 and C-20) cured for 21 days in an aggressive ammonium nitrate solution. Table 3 shows the partial and total porosity results before and after the leaching test. In both cases, the total porosity of the cement matrices (C-0 and C-20) underwent a significant increase from 20.7 to 52.7% and from 26.2 to 48.3%, for C-0 and C-20, respectively. The inverse relationship between porosity and mechanical strength is well known, as demonstrated above in section 3.3. According to the distribution density curves shown in Figure 9, both cements presented a similar distribution density of pore sizes before the leaching test (0 days but previously cured for 28 days in standardized conditions), clearly identifying a well-defined maximum at 0.025μm. After the leaching test (21 days), this maximum was converted into different maxima, which were localized in a wide range of pore sizes (5 and 0.01μm).

When the partial properties were calculated for different pore-size ranges (Table 4), it was observed that most of the pore sizes ranging between 5 and 0.1 micron were affected by the calcium-ion leaching process at 21 days, increasing their porosity by about 24-25% when compared to 0 days exposure. According to Mindess et al (Mindess et al., 2002), this range is classified as large capillary pores, which directly affect the decrease in strength and the increased permeability. However, the pore interval between 0.1 and 0.01μm (medium capillary pores next to the gel pores) was less damaged by the leaching process than in the former case. Despite this, a 57.3% increase of partial porosity was detected in C-0; while in the case of C-20, a 23% reduction of the partial porosity was observed.

3.5. Impact assessment

The replacement of 20% of OPC by ACMW reduced the CO2 emissions of the product by up to 12%, as shown in Figure 10. An estimated reduction in fossil resources of approximately 19% was achieved as a consequence of the 20% replacement of OPC, given that no additional thermal energy was needed for the valorization of the ACMW. The relative LCIA results are shown in Figure 11. All impact categories under evaluation showed a reduction in environmental impact through the substitution of 20% OPC.

The results, in the case of the ACMW, rely on key assumptions. Nevertheless, this study can provide a useful estimation of the improvement in environmental performance when this material is used in cement blends.

4. Conclusions

The leaching process in both OPC (C-0) and cements containing 20% ACMW (C-20) has produced modifications in their structures and has had various effects on the performance of the blends. In general terms, the cement matrix has shown an increase in porosity, as a consequence of increased pore sizes. A decrease in gel pores could be observed, which was attributed to the higher polymerization of the gel. Calcium leaching in C-20 decreased due to the pozzolanic effect, while the leaching of K and Mg increased due to the presence of phyllosilicates. Further partial conclusions are as follows:

1. On the basis of the evolution of the initial seven days, it can be concluded that C-20 showed no improvement in its resistance to calcium leaching when exposed to the accelerated method. However, two weeks after the accelerated exposure, the C-20 appeared to show higher resistance against the dissolution of calcium ions.
2. At the end of calcium leaching exposure, both cement matrices, C-0 and C-20, experienced similar flexural and compressive strength losses of around 85%. The loss of mechanical strength of C-20 was less than in the case of C-O. Therefore, the 20% ACMW addition slightly improved the performance of the cement pastes during the calcium-leaching processes.
3. Partial and total porosity increased in both C-0 and C-20 after 21 days of exposure. The pore range, mostly affected by the decalcification process, was between 5μm and 0.1μm (larger capillary pores) followed by pore intervals of between 0.1 and 0.01μm (medium capillary pores next to the gel pores)
4. The XRD studies showed that $Ca(OH)_2$ and $C_6AS_3H_{32}$ constituted the major hydrated phases. C_4AH_{13} was dominant in C-20, while $C_4A\overline{C}H_{12}$ prevailed in C-0.

The aggressive treatment produced a progressive decrease in $Ca(OH)_2$, $C_6AS_3H_{32}$, and $C_4A\overline{C}H_{12}$, and an increase in $CaCO_3$, and $C_3ASO_4Ca12H_2O$.

5. The surfaces became porous and the edges of the crystals were poorly defined. The leached material was deposited in the holes formed on the degraded surface. C-20 initially presented a more polymerized gel and was less modified by the leaching process than C-0, where the degradation was more pronounced.
6. In general terms, and at all times on the basis of this accelerated method, it can be concluded that the incorporation of ACMW into binary cements might induce a slight improvement in the calcium leaching phenomena. All in all, the correlation between real calcium leaching conditions and accelerated testing conditions will require further research.

Acknowledgements

This research was developed in the framework of the MATCON Associated Unit (CSIC-Tecnalia, Madrid, Spain) with the support of the Spanish Ministry of Economy and Competitiveness (Project Ref. MAT2012-37005-CO3-01/02/03) and the European Regional Development Fund (MINECO/FEDER) (Project Ref.BIA2015-65558-C3-1,2,3-R. The authors are also grateful to the Sociedad Anónima Hullera Vasco-Leonesa and to the Spanish Cement Institute (IECA) for providing us with raw materials.

References

Berner, U.R., 1988. Modeling the incongruent dissolution of hydrated cement materials. Radiochim; 44/45, 387-393.

Bjornstom, J., Martinelli, A., Matic, A., Borjesson, L, Panas. I., 2004. Accelerating effects of colloidal nano-silica for beneficial calcium–silicate–hydrate formation in cement. Chemical Physics Letters 392, 242-248.

ELCD 3.2, 2015. European reference Life-Cycle Database, Available at: http://eplca.jrc.ec.europa.eu/ELCD3/index.xhtml?stock=default [Accessed Feb. 6, 2018].

Frías, M., Sánchez de Rojas, M.I., Lúxan, M.P., 1991. Determination of specific surface area by the laser diffraction technique-comparation with the Blaine permeability method. Cem. Concr. Res. 21, 709-717.

Frías, M., Vigil de la Villa, R., Sanchez de Rojas, M.I., Medina, C., Juan, A., 2011. Scientific aspects of kaolinite based coal mining wastes in a pozzolan/Ca(OH)2 system. J. Am. Ceram. Soc. 95(1) 386-391.

Frías, M., Sanchez de Rojas, M.I., García, R., Juan, A., Medina. C., 2012. Effect of the activated coal mining wastes on the properties of blended cement matrixes. Cem. Concr. Comp.34, 678-683.

Frías, M., Rodríguez, O., Vigil de la Villa, R., García, R., Martínez-Ramírez, S., Fernandez Carrasco, L.J., Vegas. I., 2016. The Influence of Activated Coal Mining Wastes on the Mineralogy of Blended Cement Pastes. J. Am. Ceram. Soc. 99 (1) 300-307.

Gaitero, J.J. Campillo, I. Guerrero, A., 2008. Reduction of the calcium leaching rate of cement paste by addition of silica nano particles. Cem. Concr. Res. 38 (1) 112-1118.

García, R. Vigil de la Villa, R. Frías, M. Rodriguez, O. Martínez-Ramírez, S. Fernández-Carrasco, L. de Soto, I.S. Villar-Cociña. E., 2015. Mineralogical study of calcined coal waste in a pozzolan/Ca(OH)2 system. Applied Clay Science 108, 45-54.

Gerard, B., 1997. Contribution des couplages mechanique-chimie-transfer dans la tenue à long terme des ouvrages de stockage des dèchets radioactifs. PhD Thesis, ENS Cachan,

France.

Guinée, J.B. et al., 2002. Handbook on life cycle assessment. Operational guide to the ISO standards. I: LCA in perspective. IIa: guide. IIb: Operational annex. III: Scientific background., Kluwer Academic Publishers.

Goñi, S. Frías, M. Vigil de la Villa, R. Vegas. I., 2013. Decalcification of activated paper sludge – Fly ash-Portland cement blended pastes in pure water. Cem. Concr. Comp. 40, 1-6.

ISO 14040, 2006. ISO 14040:2006 (EN). LCA Principles and framework. The International Journal of Life Cycle Assessment, 2006(7), pp.652–668. Available at: http://www.springerlink.com/index/10.1007/s11367-011-0297-3 [Accessed Feb. 6, 2018].

Heukamp, F.H.,2002. Chemomechanics of calcium leaching of cement-based materials. PhD Thesis, M.I.T., USA.

Juenger, A.M.C.G., Siddique. R., 2015. Recent advances in understanding the role of supplementary cementitious materials in concrete. Cem. Concr. Res.78, 71-80.

Malhotra, V., 2000. Role of supplementary cementing materials in reducing greenhouse gas emissions. In O. Gjorv & K. Saka, eds. Concrete technology for a sustainable development in the 21st century. London: E&FN Spon, 225–35.

Medina, C. Frías, M., Sánchez de Rojas, M.I., 2014. Leaching in concretes containing recycled ceramic aggregate from the sanitary ware industry. J. Clean Prod. 66, 85-91.

Marchese García, A., 2004. Consumo de energía en operaciones de conminución de minerales. Revista minera, 322.

Mollah M.Y.A., Yu W., Schennach R., Cocke D.L., A 2000. Fourier transform infrared spectroscopic investigation of the early hydration of Portland cement and the influence of sodium lignosulfonate. Cem. Concr. Res 30, 267-273.

Mindess, S. Francis, J. Darwin. D., 2002. Concrete (2 Edition). Prentice Hall, New York (USA). 644.

Mulugeta, M. Engelsen, C.J. Wibetoe, G. Lund. W., 2011. Charge-based fractionation of oxyanion forming metals and metalloids leached from recycled concrete aggregates of different degrees of carbonation: a comparison of laboratory and field leaching test. Waste Manage. 31, 253-258.

Nakanishi, E.Y., Frías, M., Santos, S.F., Rodríguez, M.S., Vigil d ela Villa, R., Rodríguez, O., Savastano, H., 2016. Investigating the posible usage of elephant grass to manufacture the eco-friently binary cements. J. Clean. Prod. 116, 236-243.

Phung, Q.T., 2015. Effects of Carbonation and Calcium Leaching on Microstructure and Transport Properties of Cement Pastes, in: Department of Structural Engineering, Ghent University, Belgium.

Rashad, A. M., 2013. Metakaolin as cementitious material: History, scours, production and composition –A comprehensive overview. Construction and Building Materials. 41, 303–318.

Richardson, I.G. Groves, G.W., 1992. Models for the composition and structure of calcium silicate hydrate (CSH) gel in hardened tricalcium silicate pastes. Cem. Concr. Res. 22(6) 1001-1010.

Sáez del Bosque, B.I.F., Martínez-Ramírez, S., Blanco Varela, M.T., 2014. FTIR study of the effect of temperature and nanosilica on the nanostructure of C–S–H gel formed by hydrating tricalcium silicate. Construct. Build. Mater. 52, 314-323.

Saito, H., Nakane, S., Ikari, S., Fujiwara. A., 1992. Preliminary experimental study on the deterioration of cementitious materials by an acceleration method. Nucl. Eng. Des. 138 (2) 151-155.

Santamaría, A., Rojí, E., Skaf, M., Marcos, I., González, J.J. 2016. The use of steelmaking slags and fly ash in structural mortars. Construction and Building Materials; 106, 364-73.

Taylor, H.F.W., 1997. Cement Chemistry, Thomas Telford, London.

Taylor, H.F.W., 1986. Proposed structure for calcium silicate hydrate gel. J. Am. Ceram. Soc.69 (6) 464-467.

UNE EN 196-1. 2005. Methods of testing cement. Part 1: Determination of strength.

Vadillo Fernández, L., 1995. Manual de reutilización de residuos de la industria minera, siderometalúrgica y termoeléctrica, Instituto Tecnológico Geominero de España.

World Business Council for Sustainable Development/Cement Sustainability initiative (WBCSD/CSI), Global Cement Database on CO2 and Energy Information - 'Getting the Numbers Right', 2013.

Yu, P., Kirkpatrick, R.J., Poe, B., McMillan, P.F., Cong. X., 1999. Structure of Calcium Silicate Hydrate (C-S-H): Near, Mid, and Far-Infrared Spectroscopy. J. Am. Ceram. Soc. 82 (3) 742-48.

Captions

Fig 1. System boundary used for the LCA binary cement manufacturing

Fig 2. Evolution of ions concentration versus exposure time. It is assumed (not real measurements) that the concentration of ions at t0 is negligible.

Fig 3. Mineralogical evolution at 7 and 21 exposure days.

Fig 4. (a) Ettringite (b) Surface processes: dissolution of ettringite and formation of calcite.

Fig 5. (a) Degraded surfaces with superficial deposits (b) Laminar C3ASO4Ca12H2O.

Fig. 6. FTIR spectrum before and after the leaching in the range of 1300-800 cm^{-1}.

Fig 7. Flexural strength of C-20 and C-0.

Highlights

- ✓ The addition of ACMW to the cement slightly reduces the calcium leaching phenomena.
- ✓ The leaching process mainly affects the capillary pores.
- ✓ An aggressive solution produces a decrease in $Ca(OH)_2$, $C_6AS_3H_{32}$ and $C_4A\overline{C}H_{12}$ phases.

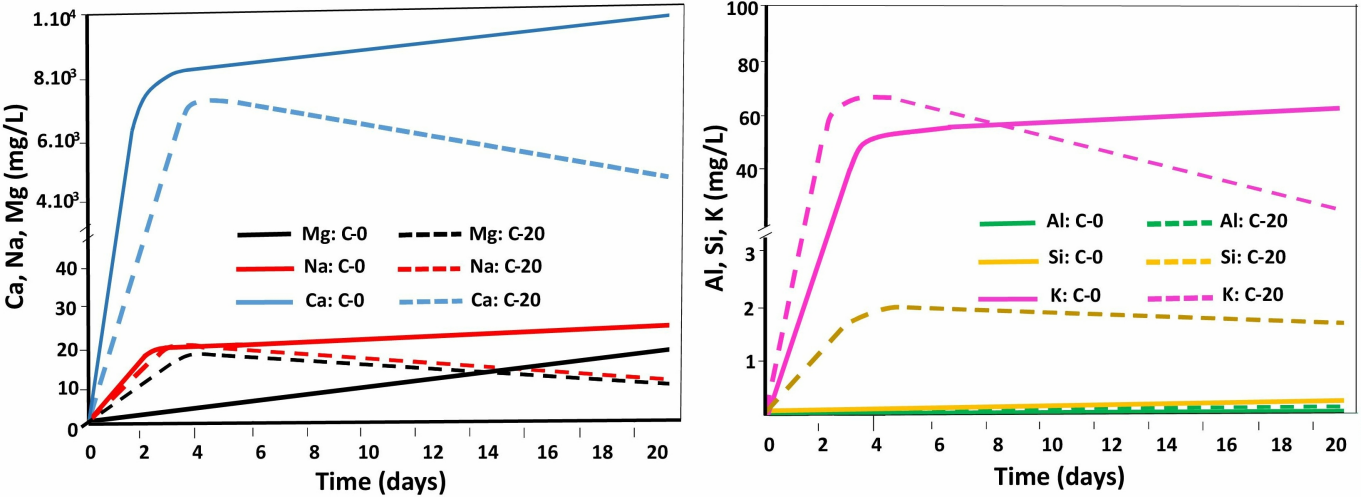
Ca, Na, Mg (mg/L)
1.10^4
8.10^3
6.10^3
4.10^3
40
30
20
10
0
Mg: C-0
Mg: C-20
Na: C-0
Na: C-20
Ca: C-0
Ca: C-20
0 2 4 6 8 10 12 14 16 18 20
Time (days)
Al, Si, K (mg/L)
100
80
60
40
3
2
1
Al: C-0
Al: C-20
Si: C-0
Si: C-20
K: C-0
K: C-20
0 2 4 6 8 10 12 14 16 18 20
Time (days)

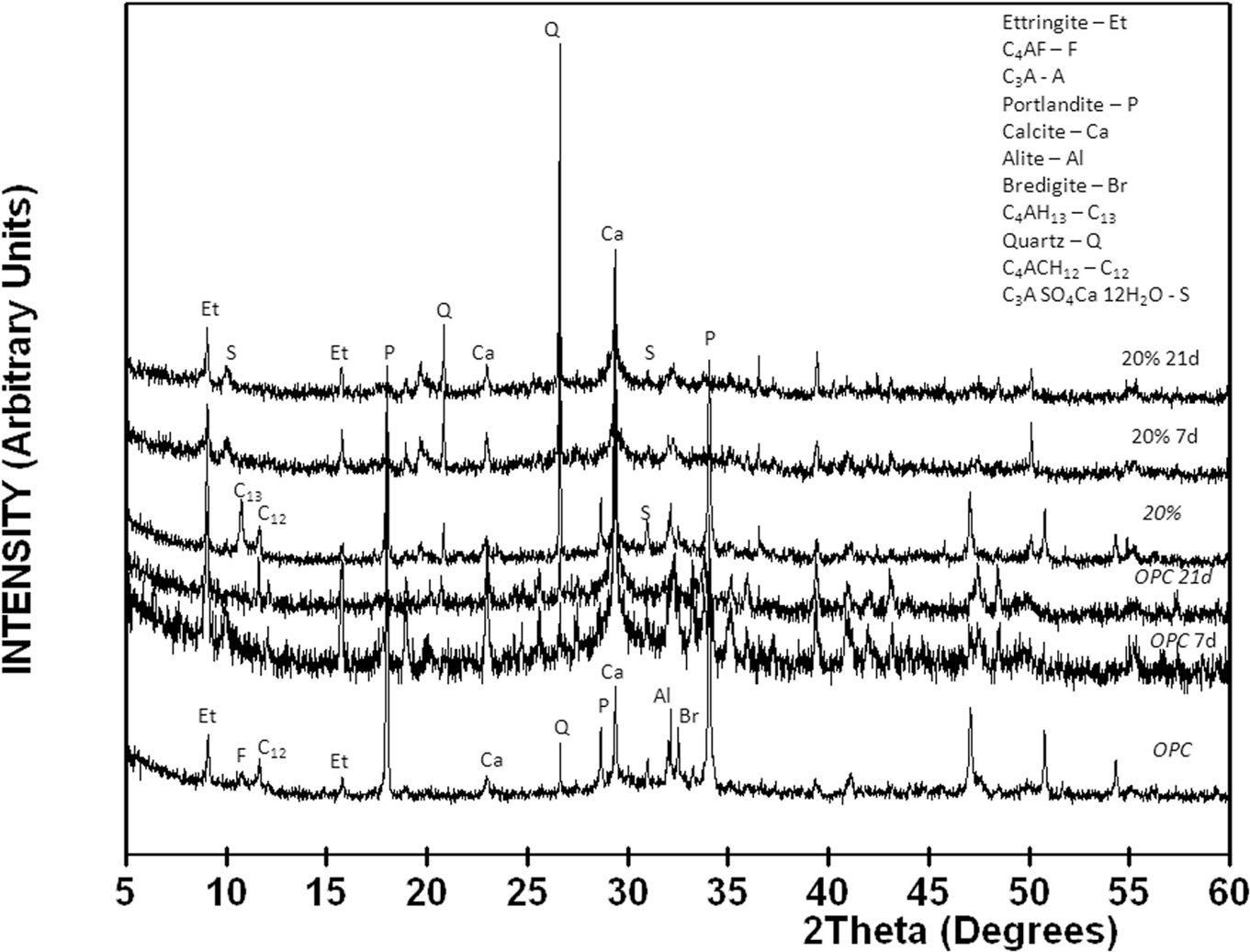
Ettringite – Et
C4AF – F
C3A - A
Portlandite – P
Calcite – Ca
Alite – Al
Bredigite – Br
C4AH13 – C13
Quartz – Q
C4ACH12 – C12
C3A SO4Ca 12H2O - S
20% 21d
20% 7d
20%
OPC 21d
OPC 7d
OPC
INTENSITY (Arbitrary Units)
2Theta (Degrees)
5
10
15
20
25
30
35
40
45
50
55
60

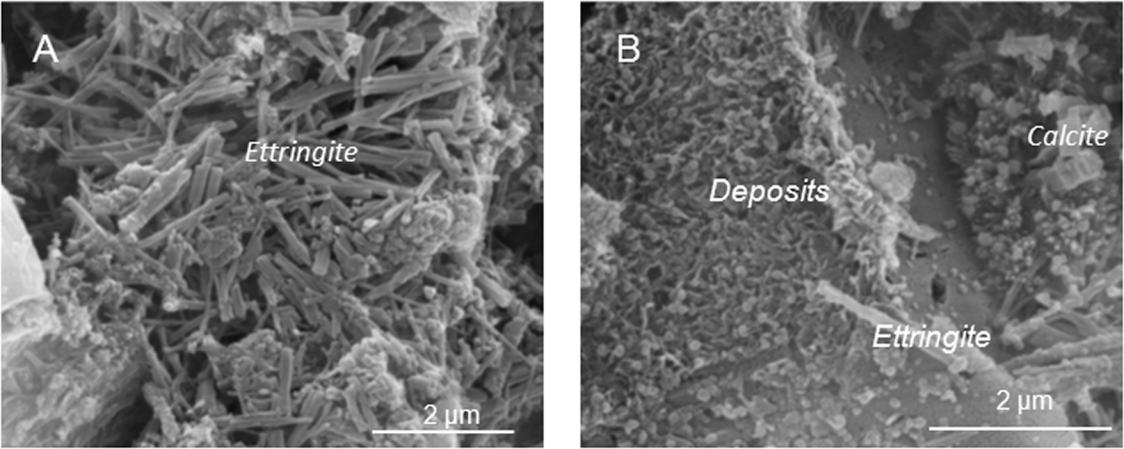
A
Ettringite
2 µm
B
Calcite
Deposits
Ettringite
2 µm

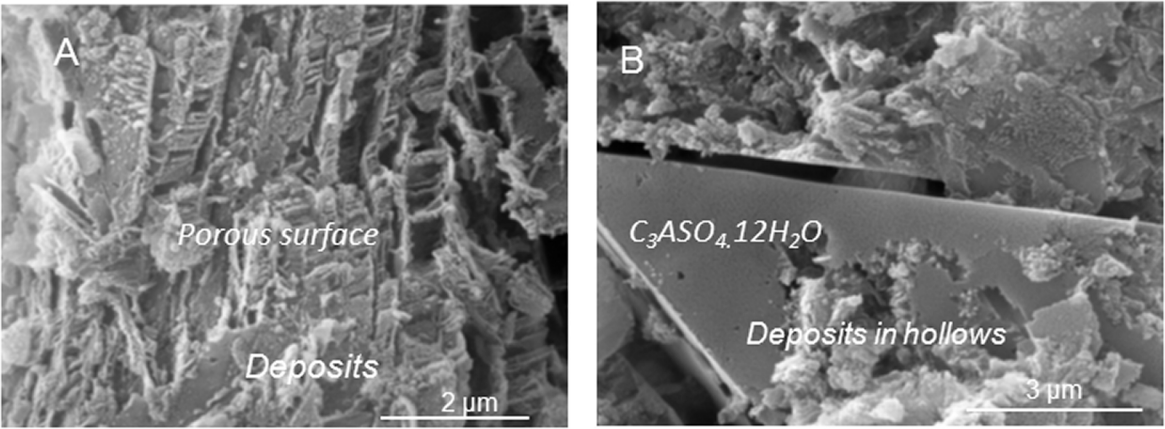
A
Porous surface
Deposits
2 µm
B
$C_3ASO_4.12H_2O$
Deposits in hollows
3 µm

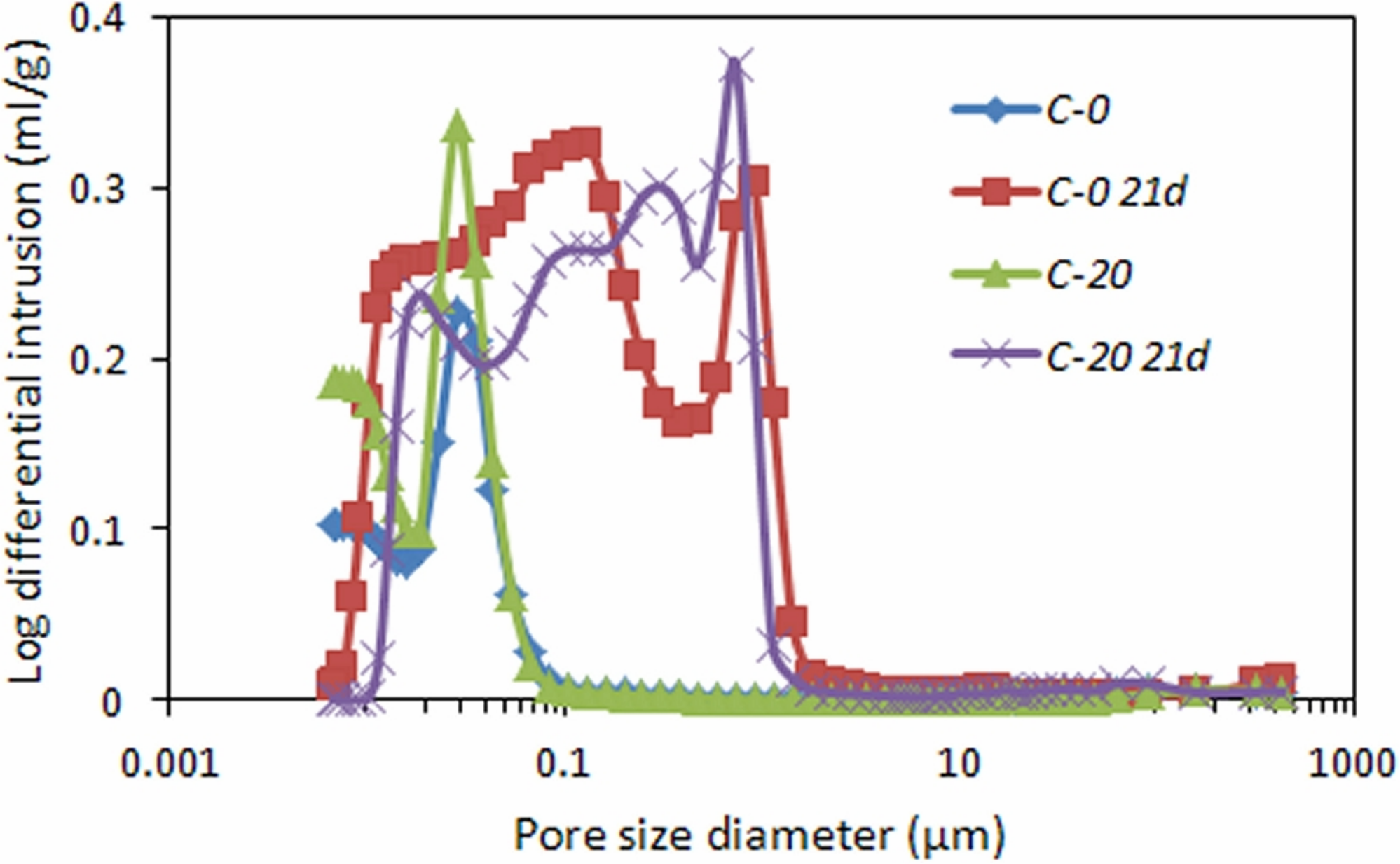
0.4
0.3
0.2
0.1
0
Log differential intrusion (ml/g)
0.001
0.1
10
1000
Pore size diameter (μm)
C-0
C-0 21d
C-20
C-20 21d

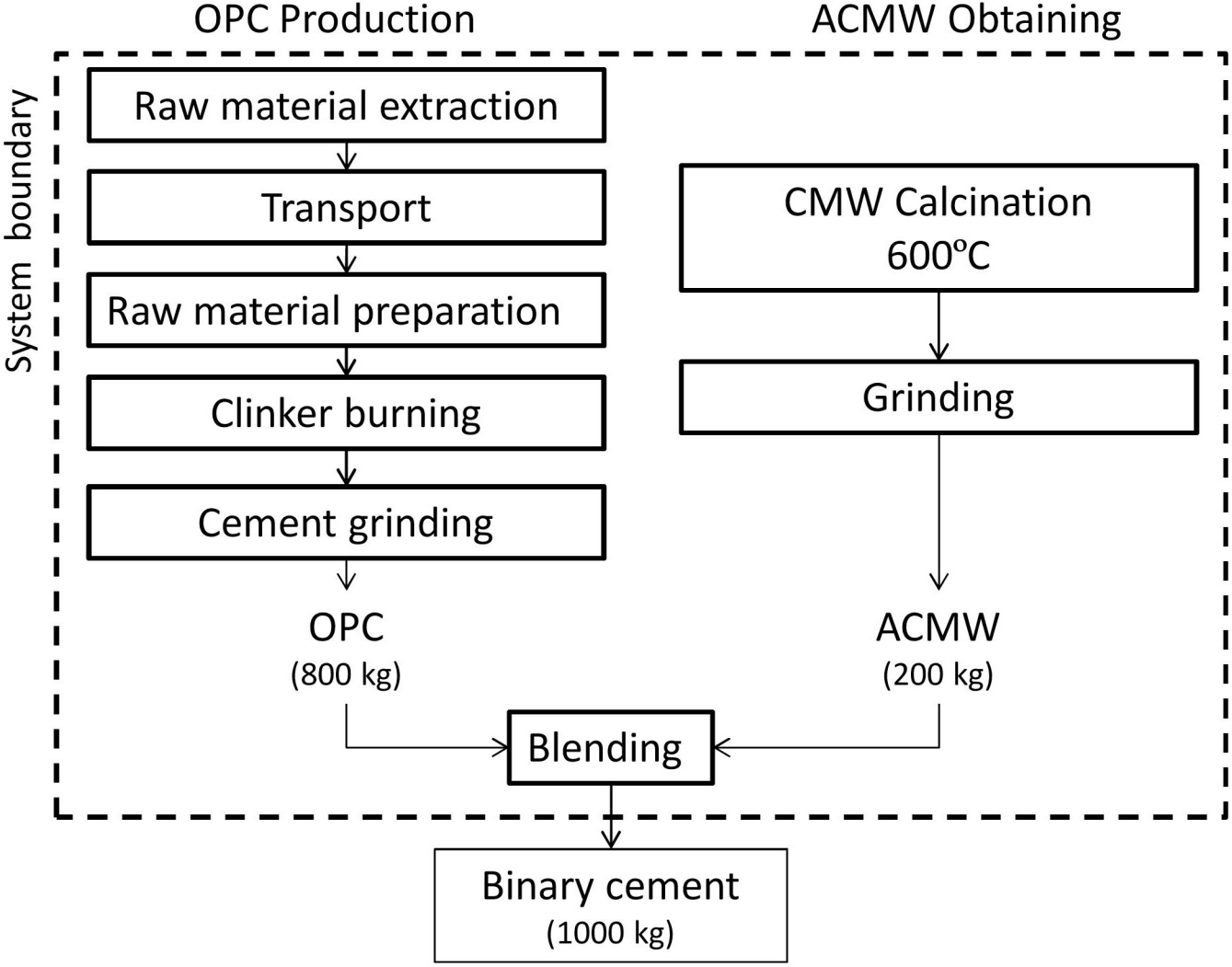
OPC Production
ACMW Obtaining
System boundary
Raw material extraction
Transport
Raw material preparation
Clinker burning
Cement grinding
CMW Calcination
600°C
Grinding
OPC
(800 kg)
ACMW
(200 kg)
Blending
Binary cement
(1000 kg)

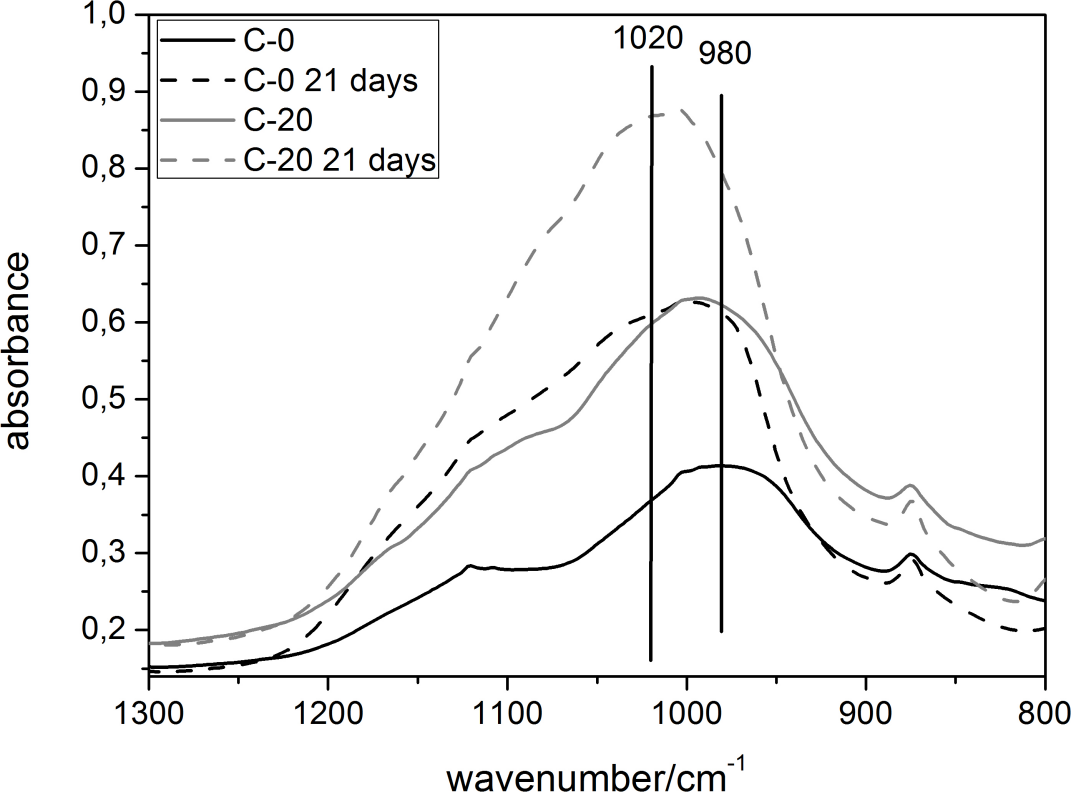
C-0
C-0 21 days
C-20
C-20 21 days
1020
980
absorbance
wavenumber/cm-1
1,0
0,9
0,8
0,7
0,6
0,5
0,4
0,3
0,2
1300
1200
1100
1000
900
800

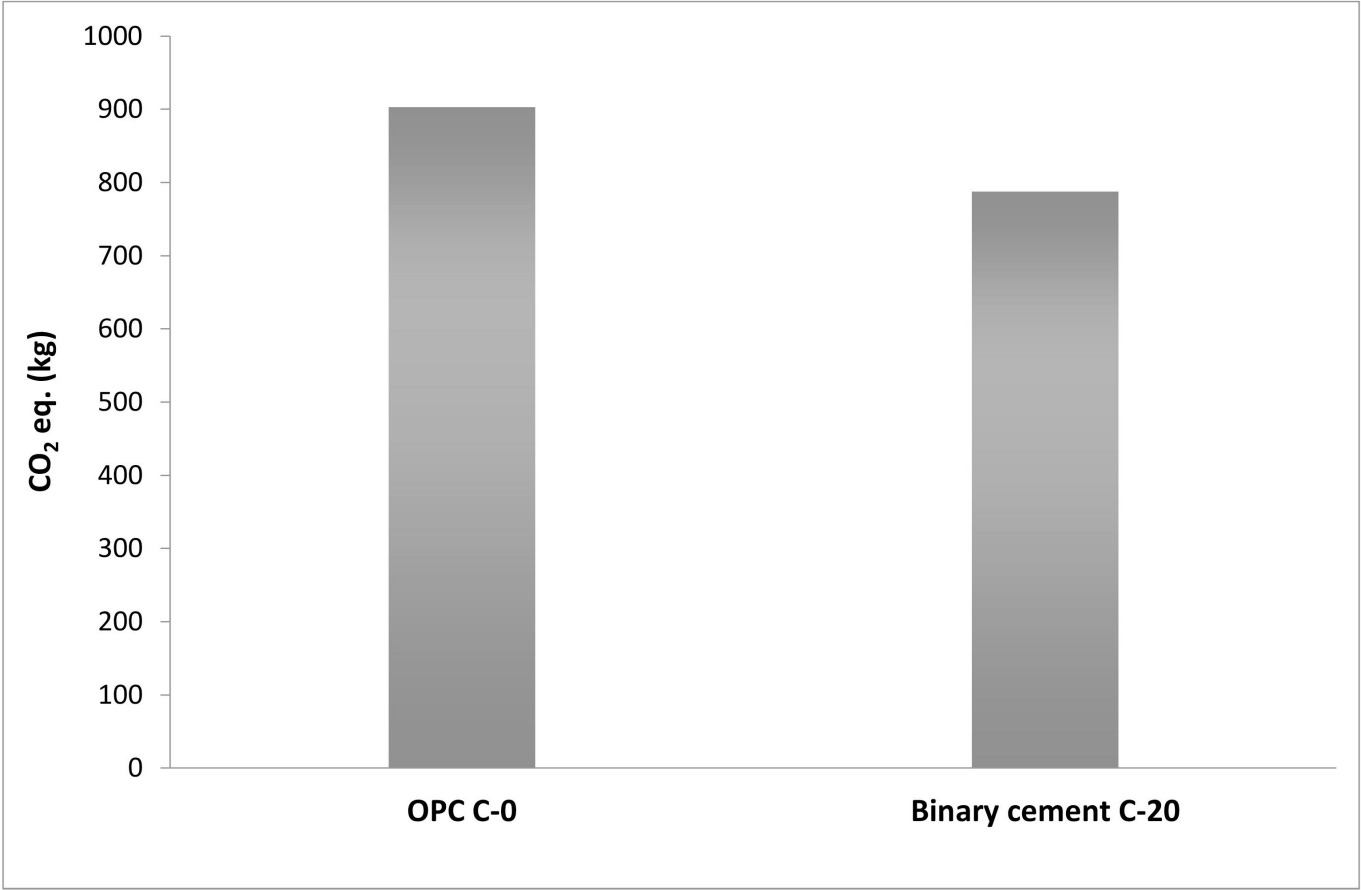
1000
900
800
700
600
500
400
300
200
100
0
CO_2 eq. (kg)
OPC C-0
Binary cement C-20

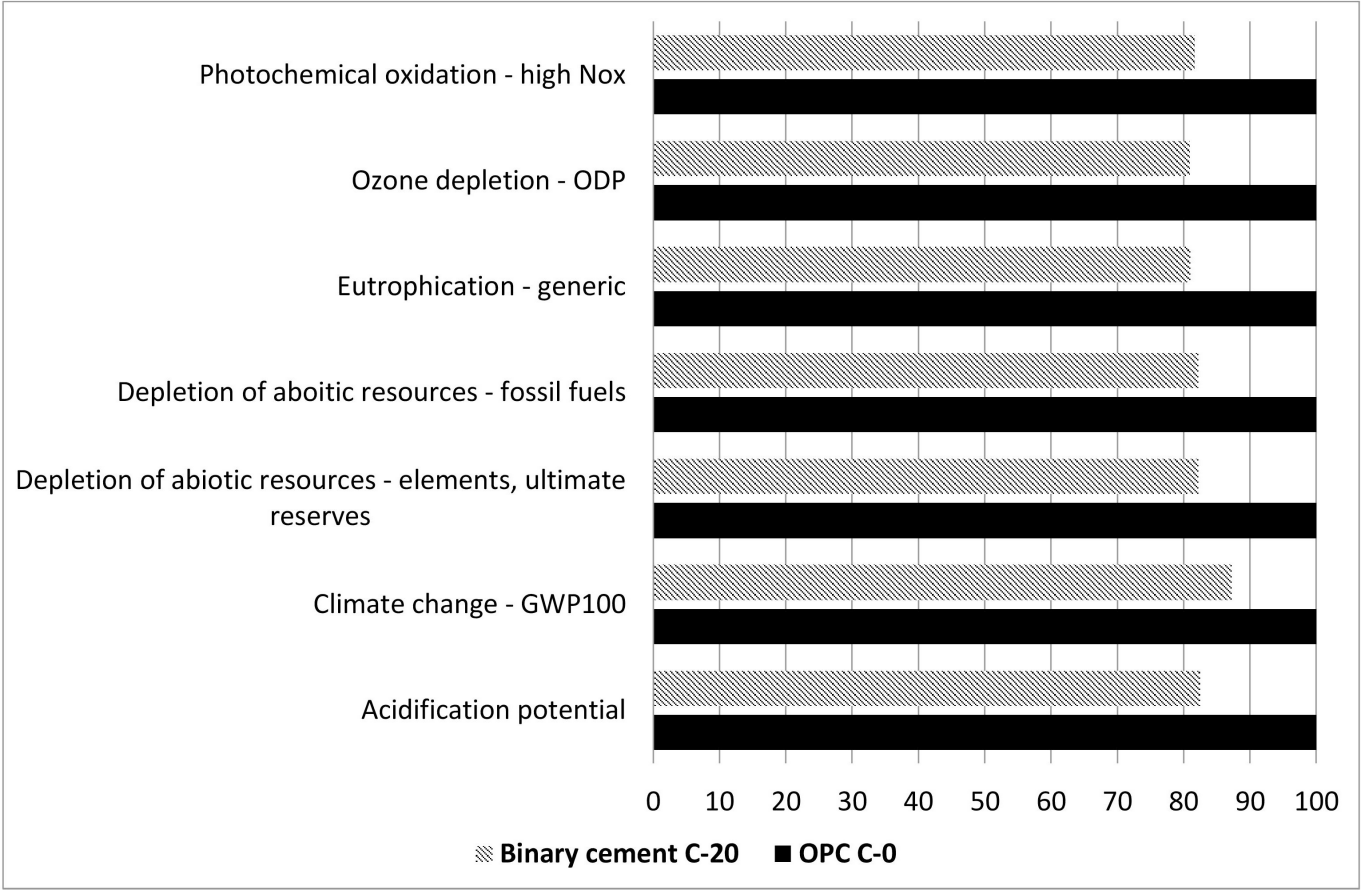
Photochemical oxidation - high Nox
Ozone depletion - ODP
Eutrophication - generic
Depletion of aboitic resources - fossil fuels
Depletion of abiotic resources - elements, ultimate reserves
Climate change - GWP100
Acidification potential
0
10
20
30
40
50
60
70
80
90
100
Binary cement C-20
OPC C-0

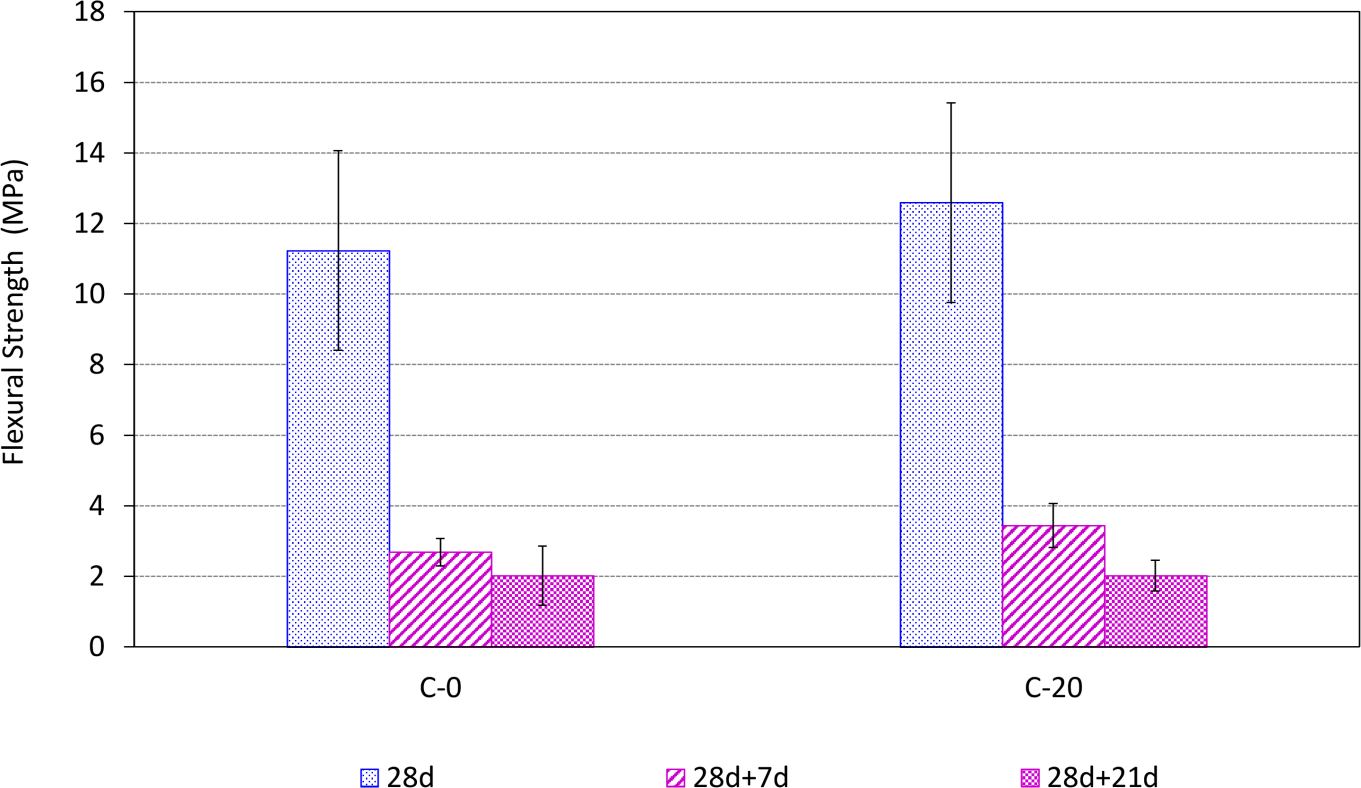
Flexural Strength (MPa)
18
16
14
12
10
8
6
4
2
0
C-0
C-20
28d
28d+7d
28d+21d

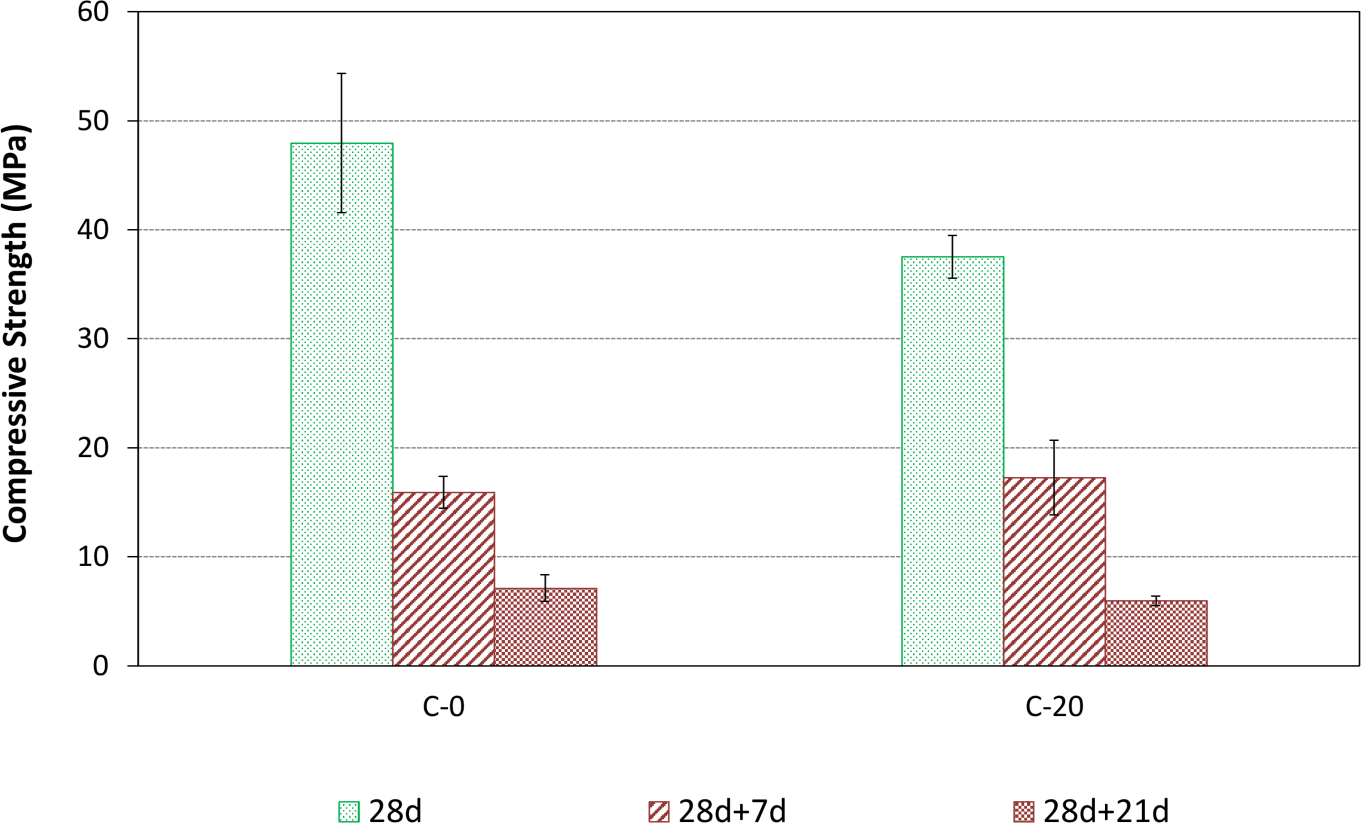
Compressive Strength (MPa)
60
50
40
30
20
10
0
C-0
C-20
28d
28d+7d
28d+21d

Table 1. Physical properties and chemical composition of the CEM I 52.5N and ACMW

	CEM I 52.5 N	ACMW
100% particles below (μm)	73	73
90% particles below (μm)	35.71	33.32
50% particles below (μm)	12.47	8.33
SiO_2	21.22	58.33
Al_2O_3	6.39	26.09
Fe_2O_3	3.19	4.64
K_2O	1.67	3.09
CaO	61.38	2.16
TiO_2	0.17	1.17
MgO	1.97	0.77
SO_3	0.42	0.27
Na_2O	0.87	0.17
P_2O_5	0.20	0.14
MnO	0.04	0.08
LOI	2.49	3.09

Table 2. Chemical compositions of cement pastes versus leaching time

Samples	SiO_2	Al_2O_3	Fe_2O_3	CaO	K_2O	TiO_2	MgO	SO_3	Na_2O	P_2O_5	LOI
C-0 0d	17.11	4.50	2.67	52.10	0.20	0.14	1.41	2.41	0.49	0.19	18.65
C-20 0d	23.81	7.99	3.05	41.91	0.62	0.24	1.30	1.94	0.44	0.17	18.44
C-0 7d	25.21	6.03	4.06	36.11	0.06	0.24	1.51	2.61	0.57	0.22	23.26
C-20 7d	30.40	10.55	4.02	28.88	0.69	0.36	1.32	1.88	0.29	0.18	21.31
C-0 21d	30.91	7.44	4.59	28.90	0.07	0.29	1.70	2.12	0.28	0.24	23.29
C-20 21d	37.69	13.17	5.02	19.09	0.79	0.52	1.42	0.49	0.14	0.19	21.35

Table 3. Evolution of Ca/Si ratio versus leaching time

Cement pastes	*C-0 0d*	*C-0 7d*	*C-0 21d*	*C-20 0d*	*C-20 7d*	*C-20 21d*
Ca/Si ratio	3.05	1.43	0.94	1.76	0.95	0.51

Table 4. Evolution of porosities versus leaching time

Cement pastes	*C-0 0d*	*C-0 21d*	*C-20 0d*	*C-20 21d*
Total (%)	20.7	52.7	26.7	48.3
		Partial porosity (%)		
5-0.1 µm	0.3	25.3	0.3	28.0
0.1-0.01 µm	16.4	25.8	24.8	19.1